January 2011

Neural Systems Of Dysfluent Reading In Childhood: Anatomical And Functional Regions Of Interest

Ava Golchin
Yale School of Medicine, avagolchin@gmail.com

Neural Systems of Dysfluent Reading in Childhood: Anatomical and Functional Regions of Interest

A Thesis Submitted to the

Yale University School of Medicine

in Partial Fulfillment of the Requirements for the

Degree of Doctor of Medicine

by

Ava Golchin

2011

Abstract

NEURAL SYSTEMS OF DYSFLUENT READING IN CHILDHOOD: ANATOMICAL AND FUNCTIONAL REGIONS OF INTEREST. Ava Golchin, John M. Holahan, Cheryl M. Lacadie, Robert K. Fulbright, Bennett A. Shaywitz. (Sponsored by Bennett A. Shaywitz.) Section of Pediatric Neurology, Department of Pediatrics, Yale School of Medicine, New Haven, CT.

Dyslexia is an unexpected difficulty in learning to read. Dyslexics experience difficulty parsing a written word's phonology. Although impairment of phonology is the cardinal feature of dyslexia, dyslexics may also be identified by slow, laborious, and inefficient reading of text (dysfluency). Dysfluent readers can be divided into those who have attained adequate skill in decoding, and those who lack both decoding accuracy and fluency. This study of 144 right handed children: (67 girls and 77 boys; ages 7-12 years, mean 9.0 years) is the first fMRI study to compare the neural pathways related to reading in dyslexics identified using dysfluency criteria. I focused my research on the design of anatomical Regions of Interest (ROIs) to compare their usefulness in localizing brain activation patterns in reading to the standard approach using functional ROIs. We hypothesize that the neural systems of reading differ in nonimpaired and dysfluent readers and that dysfluent readers who are accurate decoders may engage neural systems that differ systematically from their counterparts who are dysfluent and inaccurate decoders.

Acknowledgements

The author would like to thank Dr. Bennett Shaywitz, Dr. John Holahan, her parents, and her brother and sister.

Table of Contents

Introduction:

Dyslexia is a learning disorder defined as "a reading difficulty that is unexpected for a person's age, intelligence, level of education, or profession" (1). Dyslexia is not endemic to a particular dialect or culture; the salient features of the disorder are manifest across the spectrum of language and geography (2). Dyslexia is the most common learning disability, and aside from the reading difficulty, the population of dyslexics is heterogeneous. Dyslexia has been described and researched since the end of the 19th century, when the term was coined by the German physician P Berlin, to describe what researchers were then describing as "congenital word blindness"(3). Since that time, research on the etiology and diagnosis has been divergent and broad, encompassing topics as varied as language development, handwriting analysis, right-left confusion, light sensitivity, family pedigree analysis, verbal processing, motor sequencing, neuroanatomy, neurochemical analysis, attention deficits, and behavior. Likewise, suggestions for methods of identifying the disorder and therapeutic interventions have been varied (3). The development of neuroimaging technology in the latter part of the twentieth century has greatly influenced the direction of research and discussion on dyslexia's etiology, diagnosis, and treatment.

Dyslexics experience difficulty parsing a written word's phonology; this difficulty subsequently impedes access to higher cognitive areas related to the word's meaning (4). Reading relies on the phonological processing components of the language system that engage brain regions involved in word analysis, articulation, and form (2). Proficiency hinges on phonological awareness and disturbances in left-hemisphere posterior neural systems relevant to word decoding that are evident in fMRI analysis of dyslexic readers

(2). Data comparing nonimpaired readers to dyslexics show striking differences in neural pathways used for reading. Despite these differences, children's brains demonstrate remarkable plasticity and with guided intervention dyslexic readers may exhibit marked improvement in reading accuracy (2).

To read words efficiently, one must possess decoding *accuracy*--that is, the ability to decode the component phonemes of printed words. Skilled reading also requires *fluency*, a quick and automatic identification of the words on the page; fluency allows one to read with automaticity, prosody, and expression. Skilled readers must also comprehend vocabulary, and further, comprehend the sentence and passage as a whole. Although impairment of phonology, which impedes efficient decoding, is the cardinal feature of dyslexia, dyslexics may also be identified by slow, laborious, and inefficient reading of text (dysfluency). Dysfluent readers can demonstrate varying levels of decoding accuracy. That is, the population of dysfluent readers can be divided into those who have attained adequate skill in decoding, and those who lack both decoding accuracy and fluency.

Use of Regions of Interest in Image Based Analysis:

Region of Interest (ROI) analyses may be hypothesis driven; i.e. they involve a-priori expectations regarding brain areas involved in a task. Anatomical regions are drawn without reference to functional maps (this is thought to give an unbiased estimate of activity); however, if only a part of an ROI is activated by a task, then activation within the ROI is lost to noise by the inclusion of inactive voxels. An ROI may be subdivided, but that leads to the problem of multiple statistical comparisons being

performed on one data set. Thus, current research favors functional ROIs. Functional ROIs are derived from both a-priori hypotheses and voxel-wise analysis of images. Because there are many fewer ROIs (either anatomical or functional) than voxels, the number of statistical comparisons is reduced and, in turn, the number of multiple comparisons is reduced. The greater the number of statistical tests performed the greater chance of having false positive results. Use of ROIs rather than voxel-based analysis improves statistical power and increases the signal to noise ratio in the data.

Anatomical ROI Design Considerations:

Determining the size and shape of an ROI is important. Increasing the size of an ROI can make it difficult to pinpoint where activation exists within the ROI, and small, but important areas can be missed. Also, the entire ROI cannot be assumed to be active, and it is necessary to examine voxel-wise maps to pinpoint activity. Anatomical ROIs can be time consuming to draw, as well as subjective. I focused my research on the design of anatomical ROIs to compare their usefulness in localizing brain activation patterns to the standard approach using functional ROIs.

Hypothesis:

This is the first fMRI study to compare the neural pathways related to reading in dyslexics identified based on dysfluency, in the presence or absence of decoding deficits. We hypothesize that the neural systems of reading differ in nonimpaired and dysfluent readers (5). We conjecture that there may be diversity among dysfluent readers in that dysfluent readers who are accurate decoders may engage neural systems that differ systematically from their counterparts who are dysfluent and inaccurate decoders.

Specific Aims:

The principal aim of this study is to compare the use of anatomical ROIs relative to the standard functional ROI analyses used in fMRI.

.Methods:

Three groups of readers were identified in this study: dysfluent readers with inaccurate decoding (DFI), dysfluent readers with accurate decoding (DFA), and Non-impaired readers who are accurate decoders and fluent readers (NI).

Subject Cohort:

We studied 144 right handed children: (67 girls and 77 boys; ages 7-12 years, mean 9.0 years). A non-impaired reading (NI) group and two dysfluent (DF) reading groups were identified. Criteria for dysfluency were met if the participant achieved a Gray Oral Reading Test-IV (GORT) (7) *Fluency* standard score (the composite of rate and accuracy), or a score on either subtest or the total for the Test of Word Reading Efficiency (TOWRE) (8) below the 25th percentile. The dysfluent readers were further categorized as dyfluent with inaccurate decoding (DFI) if the Woodcock-Johnson (WJ)(9) *Basic Reading* score or the WJ *Word Attack* subtest score was < 90 (below the 25th percentile). Those dysfluent readers with WJ scores above the 25th percentile were categorized as dysfluent with accurate decoding (DFA). Non-Impaired (NI) readers attained scores on all GORT, WJ, and TOWRE measures above the above the 40th percentile. All but 1 child had either a Verbal or Full-Scale IQ above 80, as measured by the Wechsler Abbreviated Intelligence Scale (WASI) (10). The gender composition of the

three reading groups is presented in the upper portion of Table 1 and a summary of the cognitive and primary reading measures is presented in the lower portion of Table 1.

	DFI		**DFA**		**NI**	
Overall N	38		59		47	
n -Males	27		33		17	
n-Females	11		26		30	
	M	*SD*	*M*	*SD*	*M*	*SD*
AGE	9.14	0.97	9.24	1.18	8.64	1.14
WASI Full-Scale IQ	99.0	13.4	104.3	11.4	121.2	14.8
Woodcock-Johnson						
Basic Reading	86.5	3.5	96.1	4.5	118.9	11.3
Word ID	86.2	5.9	95.1	5.1	120.8	11.0
Word Attack	88.4	5.4	97.7	5.3	113.6	9.9
Gray Oral Reading Test						
Rate	5.4	2.0	6.4	1.8	13.9	2.1
Accuracy	4.4	1.9	5.2	1.8	11.9	2.9
Fluency	4.3	1.9	5.3	1.7	13.0	2.6
Comprehension	8.5	3.4	9.6	2.9	13.4	3.0
Test of Word Reading Efficiency						
Sight Words	83.9	10.8	89.8	7.1	118.2	10.0
Phonologic Decoding	80.7	5.8	87.0	5.7	113.4	10.0
Total	78.8	7.5	86.1	6.3	119.1	11.0

Table 1: Gender composition, Cognitive Ability, and Reading achievement of the three reading groups.

fMRI Tasks:

Two types of tasks were used: line orientation and rhyme judgment. For each task, the subject viewed two simultaneously presented stimulus displays, one above the other, and was asked to make a same/different judgment by pressing a response button if the displays matched on a given cognitive dimension: either line orientation (Line: eg, "Do [//\/] and [////] match?") or rhyme (the combination of Word Rhyme [WR] and Nonword Rhyme [NWR]: "Do [LEAT] and [KETE] rhyme?")

Data Acquisition:

Head positioning in the magnet was standardized using the canthomeatal landmarks. In the scanner, cushions inside the head coil were used to reduce head movement, and headphones (RTC technologies) were used to dampen the scanner noise, to communicate with participants and deliver audio components of the task. Conventional T1-weighted spin-echo sagittal anatomical images were acquired for slice localization using a 1.5T whole body imaging system with a quadrature head coil (Sonata; Siemens AG, Erlangen, Germany). After a 3-plane localizer and a multiple-slice sagittal localizer, fourteen T-1 weighted axial slices (TR=420 ms; TE=11 ms; bandwidth=130 Hz/pixel; FA= 90°; slice thickness=7mm; FOV=200 x 200 mm; matrix=256 x 256) were obtained using flash spin-echo imaging parallel to the anterior and posterior commissure (AC–PC). Eight functional data series (four for each task) were then acquired with a single-shot gradient-echo echo planar imaging (EPI) sequence (TR=1500 ms; TE=60 ms; bandwidth=1735 Hz/pixel; FA=60°; slice thickness = 7mm; FOV=200 x 200 mm; matrix=64 x 64; images per slice=91) with same slice localizations as the anatomical.

Stimuli were projected onto a semi-transparent screen at the head of the bore, viewed by the subject via a mirror mounted on the head coil. At the end of the functional imaging, a high resolution 3D Spoiled Gradient Recalled Acquisition in the Steady State (SPGR) T1-weighted sequence (TR = 24 ms; echo time (TE) = 4.73 ms; bandwidth=130 Hz/pixel; flip angle (FA) = 45°; slice thickness=1.5mm; field of view=240 x 240 mm; matrix=256 x 256) was used to acquire sagittal images for multi-subject registration.

Imaging Data Analysis:

All data were converted from Digital Imaging and Communication in Medicine (DICOM) format to analyze format using XMedCon (11). During the conversion process, the first six images at the beginning of each of the eight functional series were discarded to enable the signal to achieve steady-state equilibrium between radio frequency pulsing and relaxation leaving 85 images per slice per trial for analysis. Functional images were realigned (motion-corrected) with the Statistical Parametric Mapping 99 algorithm (www.fil.ion.ucl.ac.uk/spm/software/spm99) for three translational directions (x, y or z) and three possible rotations (pitch, yaw or roll). Trials with linear motion that had a displacement in excess of 2 mm or rotation in excess of 3° were rejected. Individual subject data was analyzed using a General Linear Model (GLM) on each voxel in the entire brain volume with regressors specific for each task. For the Rhyme task there were regressors for the real-word rhyming task and the non-word rhyming task (relative to a control task of slanted lines). The resulting functional images for each task were spatially smoothed with a 6 mm Gaussian kernel to account for variations in the location of activation across subjects. The output maps were normalized beta-maps, which were in the acquired space (3.125mm x 3.125mm x 7mm).

Image Registrations:

To take these data into a common reference space, three registrations were calculated within the Yale BioImage Suite software package.(12) The first registration performs a linear registration between the individual subject raw functional image and that subject's 2D anatomical image. The 2D anatomical image is then linearly registered to the individual's 3D anatomical image. The 3D differs from the 2D in that it has a 1 x 1 x 1 mm resolution whereas the 2D z-dimension is set by slice-thickness and its x-y dimensions are set by voxel size. Finally, a non-linear registration is computed between the individual 3D anatomical image and a reference 3D image. The reference brain used was a single control child's high resolution anatomical that was manually stripped to remove all skull and meninges. All three registrations were applied sequentially to the individual normalized beta-maps to bring all data into the common reference space. A radiologist manually identified the AC, PC, two mid-sagittal points and the bounding box of the reference brain which consisted of six boundary points: superior, inferior, anterior, posterior, right lateral and left lateral. These points were then used to create a piecewise-linear mapping into Talairach space.

Anatomical ROI Analysis Protocol:

Using BioImageSuite Software, I imported single subject brain scans, and reoriented them to match the axial reference brain. The skull was removed from the three dimensional image using a brain extraction software tool in a two-step series. The first extraction served to remove throat, and neck and most of the skull from the image data; the second extraction step more removes more precisely any remaining skull and

meninges. A successfully extracted brain was then cropped to reduce free space in the image, and to reduce registration time. An interactive registration tool was used to align different images of the same brain. Registrations were as follows: 2D conventional thick slice anatomical with 3D wholebrain anatomical; 4D echoplanar to 2D conventional thick slice anatomicals; reference 3D brain with the individual subject's 3D brain. 2D to 3D linear registrations, as well as 3D to reference non-linear registrations were verified, and inaccurate registrations were manually transformed. Activation maps were created to give a visual representation of results, and the result maps were overlayed onto a reference space with a reference brain. Composite maps of subjects were created using the BrainRegister and DualMultiSubject programs within the BioImageSuite package.

Anatomical

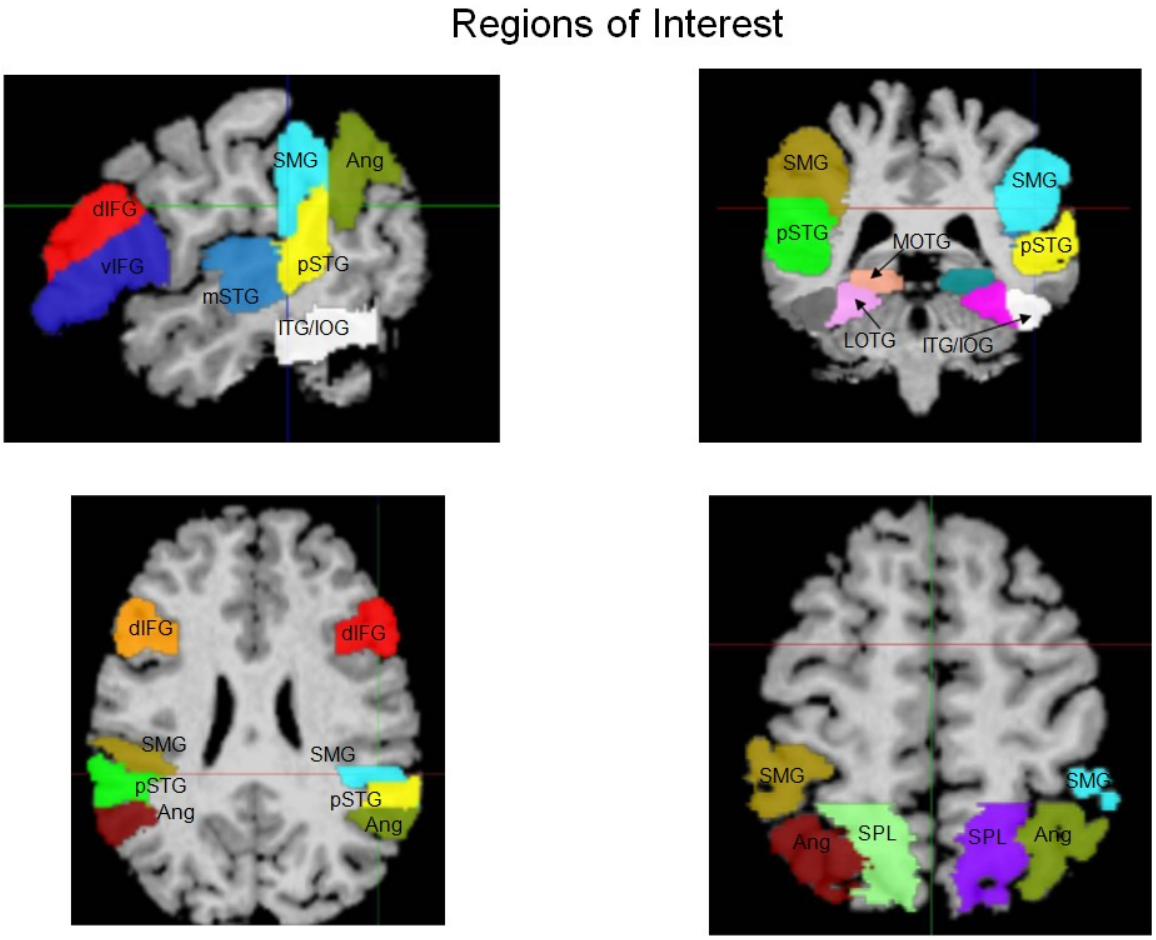

Gyrus	Name
Ang	Angular Gyrus
SMG	Supramarginal Gyrus
pSTG	posterior Superior Temporal Gyrus
mSTG	middle Superior Temporal Gyrus
ITG/IOG	Inferior Temporal Gyrus/Inferior Occipital Gyrus
vIFG	ventral Inferior Frontal Gyrus
dIFG	dorsal Inferior Frontal Gyrus
MOTG	Middle Occipital Temporal Gyrus
LOTG	Lateral Occipital Temporal Gyrus
SPL	Superior Parietal Lobule

Figure 1. Anatomical Regions of Interest designed for this study.

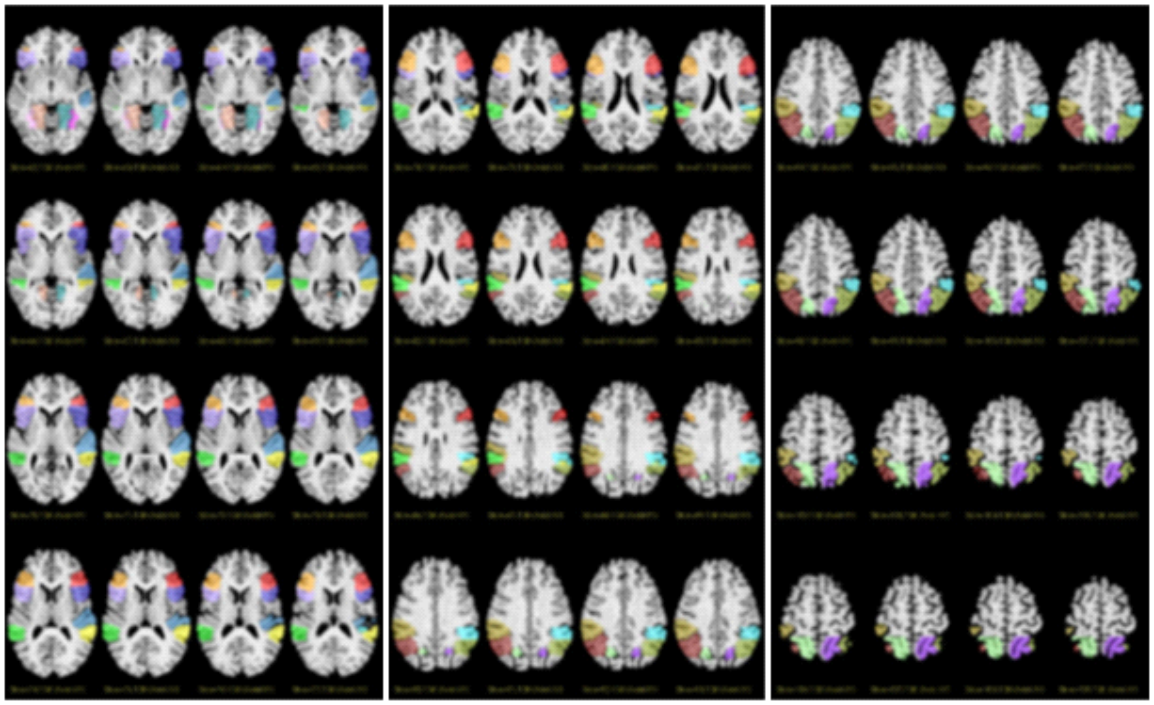

Figure 2. A single ROI required that tracing be performed on ~120 slices in a combination of axial, coronal and sagittal planes. The process was repeated for each ROI. Above are examples of Anatomical ROIs displayed in the axial plane.

Analysis of Reading Group Differences:

Functional ROI:

The dependent variable for each functional ROI is a normalized mean intensity averaged across all voxels within the ROI for each subject. For group comparisons, mean ROI activations across all subjects within each group were submitted to a single factor ANOVA with reading group (DFI, DFA, or NI) serving as the single factor and $p <= .05$ as the criterion for overall statistical significance. Ten separate ANOVA were performed, two for each of five functional regions retained for analysis. One for the left hemisphere and the second for the corresponding region in the right hemisphere. Tukey HSD post-hoc pairwise group comparisons were used to identify the sources of statistical

significance among the three reading groups. Five functional ROIs were selected for detailed analysis: Middle Frontal Gyrus (Brodmann Area [BA] 10), Inferior Occipital Gyrus (BA19), Middle Temporal Gyrus (BA 21), Anterior Inferior Parietal Lobule (BA39), Inferior Frontal Gyrus (Broca's Area – BA 44 & 45).

Anatomical ROI:

The dependent variable for each Anatomical ROI is the raw (non-normalized) mean intensity averaged across all voxels within the ROI for each subject. For group comparisons, mean ROI activations across all subjects within each group were submitted to a single factor ANOVA with reading group (DFI, DFA, or NI) serving as the single factor and $p <= .05$ as the criterion for overall statistical significance. Twenty separate ANOVA were performed, two for each of the ten Anatomical regions. One for the left hemisphere and the second for the corresponding region in the right hemisphere. Tukey HSD post-hoc pairwise group comparisons were used to identify the sources of statistical significance among the three reading groups in each analysis.

Results:

As can be seen in Table 1, there are more boys than girls in the dysfluent groups (DFI and DFA). The overall difference in gender composition of the groups is statistically significant (Fisher's exact test $\chi 2\ (2) = 17.953$, $p < .001$). Similarly, a one-way ANOVA for age reveals an overall difference among the three groups for age ($p < .021$), with DFA being older than their NI peers ($p = .018$) in the only statistically significant Tukey HSD pairwise post-hoc comparison.

As would be expected, the three reading groups differ significantly ($p < .001$) in overall ANOVA comparisons on all cognitive measures. In pairwise comparisons, the NI group achieves higher scores than both the DFA and DFI groups ($p < .001$) on all cognitive measures. Similarly the DFI and DFA groups differ significantly ($p < .001$) on the three WJ reading measures, Phonologic Decoding subtest and Total Score of the TOWRE. For the GORT, the DFA group attained significantly higher scores for Rate ($p = .037$) and exhibited a trend toward higher scores on Fluency ($p = .062$), however, the DFA and DFI groups do not differ significantly with respect to Accuracy or Comprehension.

Group activations:

As an aid for interpreting differences between the reading groups, a summary of group activations for the Non-Word Rhyming task are presented as composite maps in Figure 3.

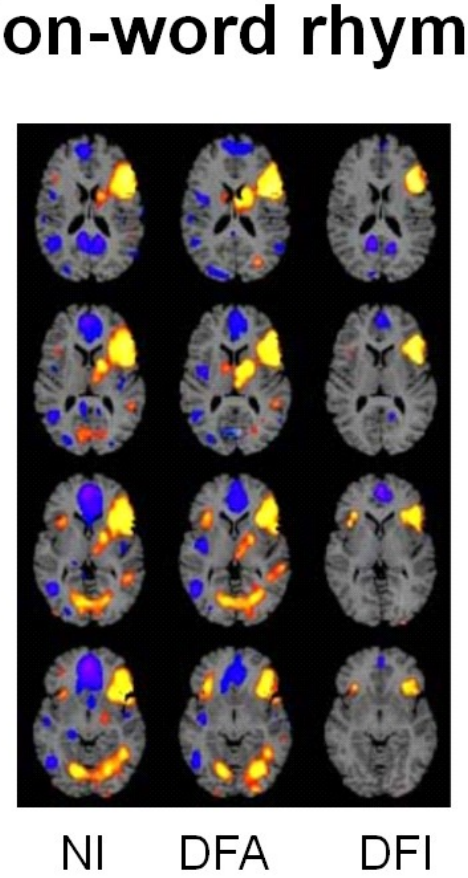

Figure 3. Group averaged activations for NWR task after subtraction of Line Orientation task activations. **NI (column 1):** Activation is seen in left Inferior Frontal Gyrus, bilateral Middle Frontal Gyrus, left Superior Temporal Gyrus, left globus pallidus, left putamen, left thalamus, left anterior cingulate, left Superior Frontal Gyrus, bilateral lingual gyrus, and in left angular gyrus. **DFA (column 2):** Activation is seen in bilateral Inferior Frontal Gyrus, bilateral Middle Frontal Gyrus, left Superior Temporal Gyrus, bilateral globus pallidus, left putamen, right central sulcus region, bilateral lingual gyri, left middle occipital gyrus, bilateral anterior cingulate gyrus, bilateral Superior Frontal Gyrus, and left angular gyrus. **DFI (column 3):** Activation is seen is in left Inferior Frontal Gyrus, left Middle Frontal Gyrus, right central sulcus, left globus pallidus, left putamen, left anterior cingulate gyrus, and bilateral Superior Frontal Gyrus.

Reading Group comparisons:

Composite maps representing the differences between specific reading groups are presented in Figure 4.

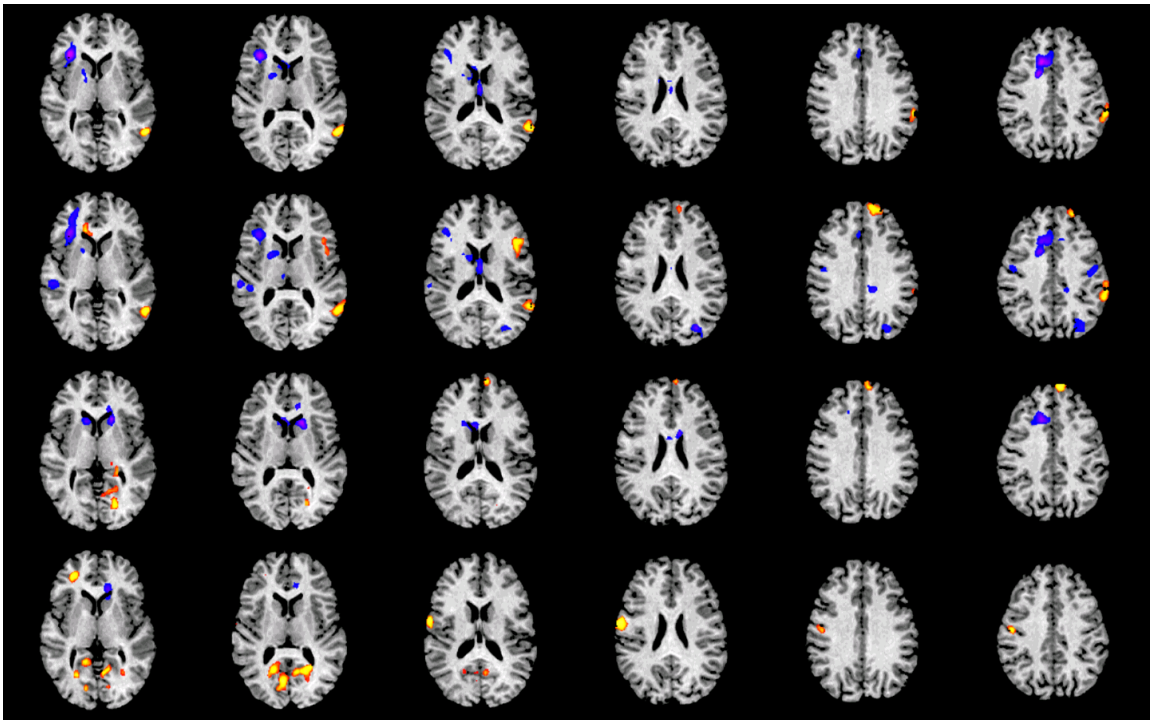

Figure 4. Composite contrast maps directly comparing the brain activation of the three groups for the Combined Rhyme tasks (Word Rhyme and Nonword Rhyme tasks taken together) with activations for the Line Orientation task subtracted out). Each row represents a specific contrast: **Row1**: NI-RD (DFI and DFA combined); **Row2**: NI-DFA **Row3**: NI-DFI, **Row4**: DFA-DFI. The six columns are axial slices in ascending order. Red-yellow indicates brain regions that were more active in the first group compared to the second; blue-purple indicates brain regions more active in the second group compared to the first. For example, in the first row (NI- RD), regions more active in NI compared to RD during the Combined Rhyme tasks are in red-yellow, and areas more active in RD compared to NI are in blue-purple.

Functional Regions:

ROI	Gyrus	*p*		*F*
		Left	**Right**	
BA 10	Middle Frontal	ns	.035	3.45
BA 19	Inferior Occipital	.007	ns	5.21
BA 21	Middle Temporal	ns	.022	3.93
BA 39	Anterior Inferior Parietal Lobule	.002	ns	6.75
BA 44 & 45	Inferior Frontal	ns	.001	6.88.

Table 2. Summary of significance of overall group differences among the three reading groups for activation in Functional ROIs. (ns = not statistically significant at $p < .05$)

A summary of the statistical significance of ten overall ANOVA is presented in Table 2. Mean and standard errors of the three reading groups for each of the statistically significant regions were plotted and post-hoc pairwise comparisons are presented in Figures 5 – 9.

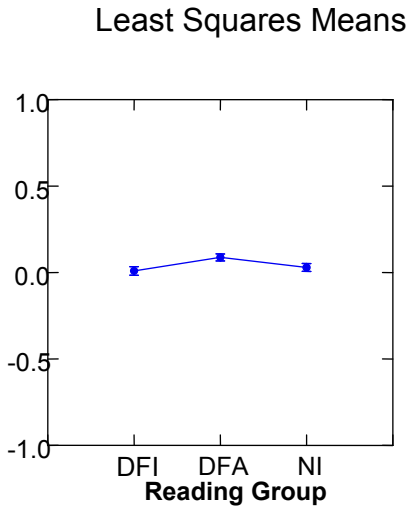

Figure 5. Mean activation in Right Hemisphere Brodmann Area 10 (Middle Frontal Gyrus). Post-hoc comparisons reveal that activation in the DFA group is significantly higher than the DFI group (p =.040). Other pairwise comparisons are not statistically significant.

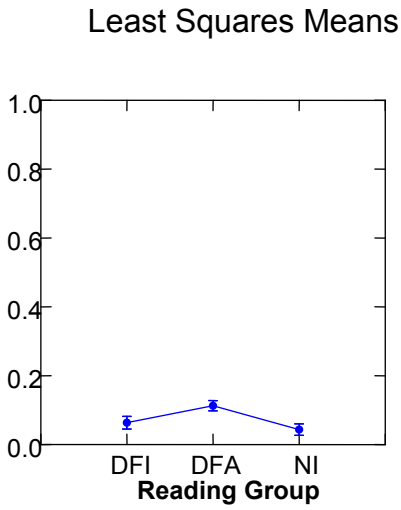

Figure 6. Mean activation in Left Hemisphere Brodmann Area 19 (Inferior Occipital Gyrus). Post-hoc comparisons reveal that the DFI and DFA groups do not differ, DFI does not differ from NI, but activation for the DFA group is significantly higher than that of the NI group (p = .005).

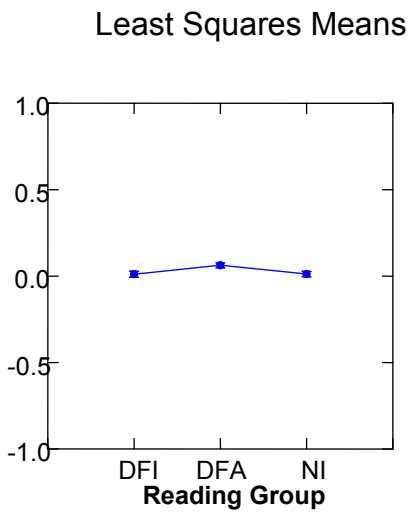

Figure 7. Mean activation in Right Hemisphere Brodmann Area 21 (Middle Temporal Gyrus). Post-hoc comparisons reveal that the activation in the DFA group is significantly higher than in the NI group (p = .043), DFI does not differ from NI, but there is a non-significant trend (p = .054) for higher activation in the DFA group than that of the DFI group.

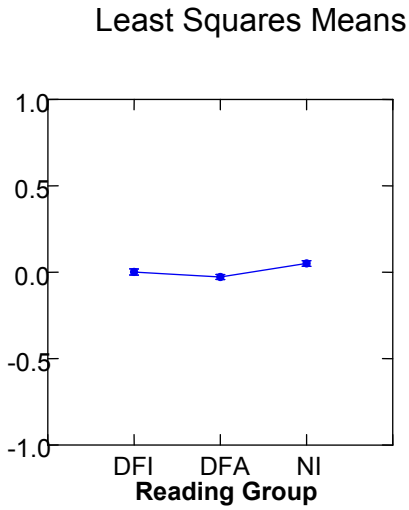

Figure 8. Mean activation in Left Hemisphere Anterior Brodmann Area 39. Post-hoc comparisons reveal that the activation in the NI group is significantly higher than in the DFA group (p < .001), DFI does not differ from NI, but there is a non-significant trend (p = .054) for higher activation in the DFI group than that of the DFA group.

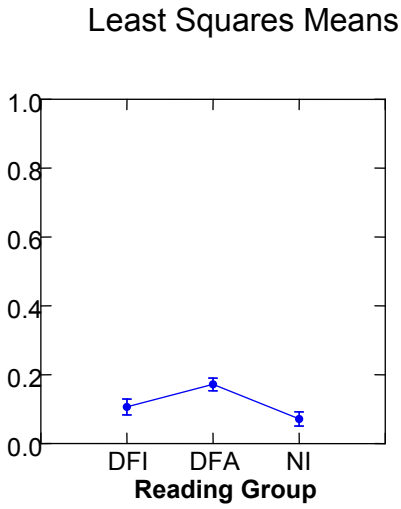

Figure 9. Mean activation in Right Hemisphere Brodmann Area 44 & 45 (Broca's Area – Inferior Frontal Gyrus). Post-hoc comparisons reveal that the activation in the DFA group is significantly higher than in the NI group ($p < .001$), DFI does not differ from NI, but there is a non-significant trend ($p = .068$) for higher activation in the DFA group than that of the NI group.

Anatomical Regions:

A summary of the statistical significance of twenty overall ANOVA is presented in Table 2. Means and standard errors of the three reading groups for each of the statistically significant regions were plotted and post-hoc pairwise comparisons are presented in Figures 10 – 11.

ROI	Gyrus	*p*		*F*
		Left	**Right**	
Ang	Angular	.091(ns)	ns	2.44
SMG	Supramarginal	.085(ns)	ns	2.52
pSTG	posterior Superior Temporal	ns	ns	
mSTG	middle Superior Temporal	ns	ns	
ITG/IOG	Inferior Temporal/Inferior Occipital	ns	ns	
vIFG	ventral Inferior Frontal	.002	ns	6.37
dIFG	dorsal Inferior Frontal	.001	ns	6.84
MOTG	Middle Occipital Temporal	ns	ns	
LOTG	Lateral Occipital Temporal	ns	ns	
SPL	Superior Parietal Lobule	.080(ns)	.085(ns)	2.47/2.51

Table 3. Summary of significance of overall group differences among the three reading groups for activation in Anatomical ROIs. (ns = not statistically significant at $p < .05$)

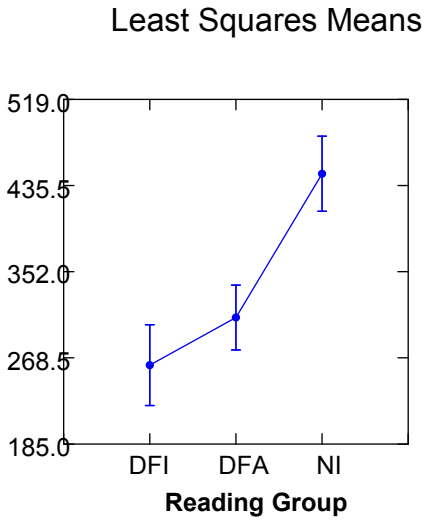

Figure 10 Mean activation in Left Dorsal Inferior Frontal Gyrus. Post-hoc comparisons reveal that the DFI and DFA groups do not differ, DFI differs from NI (p =.002), and DFA differs from NI (p = .011).

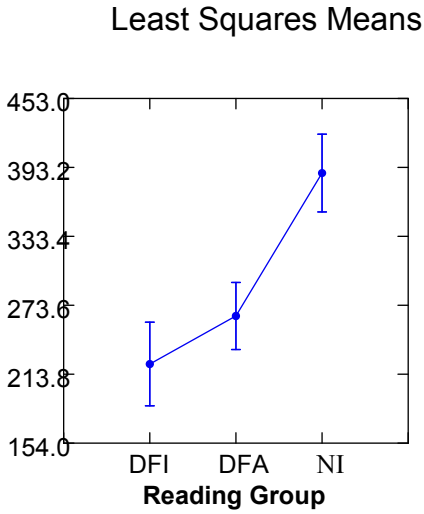

Figure 11. Mean activation in Left Ventral Inferior Frontal Gyrus. Post-hoc comparisons reveal that the DFI and DFA groups do not differ, DFI differs from NI (p =.002), and DFA differs from NI (p = .015).

Four anatomical regions approached, but did not reach, statistical significance. To summarize those non-significant trends, means and standard errors are plotted for the three reading groups and results of the post-hoc comparisons are presented in Figures 12 - 16.

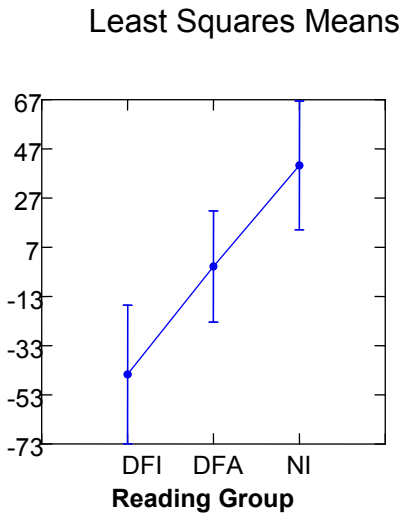

Figure 12. Mean activation in Left Angular Gyrus. Although not statistically significant, the observed difference between DFI and NI groups yielded a post-hoc $p = .069$.

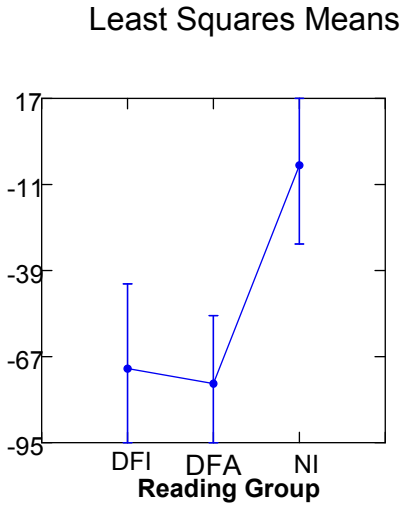

Figure 13. Mean activation in Left Supramarginal Gyrus. Although not statistically significant, the observed difference between DFI and NI groups yielded a post-hoc $p = .184$ and the observed difference between DFI and NI groups yielded a post-hoc $p = .09$.

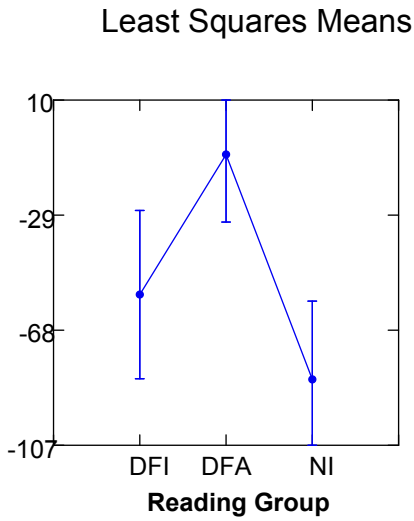

Figure 15. Mean activation in Left Superior Parietal Lobule. Although not statistically significant, the observed difference between DFA and NI groups yielded a post-hoc $p = .075$.

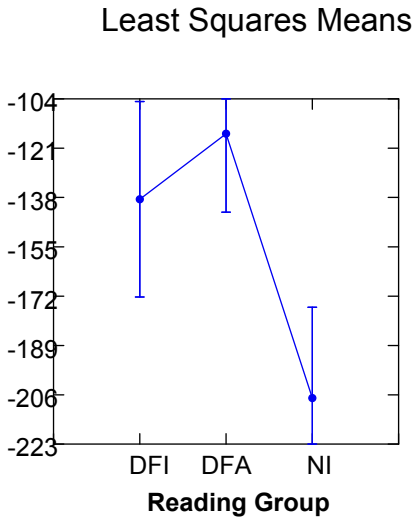

Figure 16. Mean activation in Right Superior Parietal Lobule. Although not statistically significant, the observed difference between DFA and NI groups yielded a post-hoc $p = .071$.

Summary:

The majority of the significant differences were obtained for functional ROIs and those differences distinguish the DFA group from the NI group.

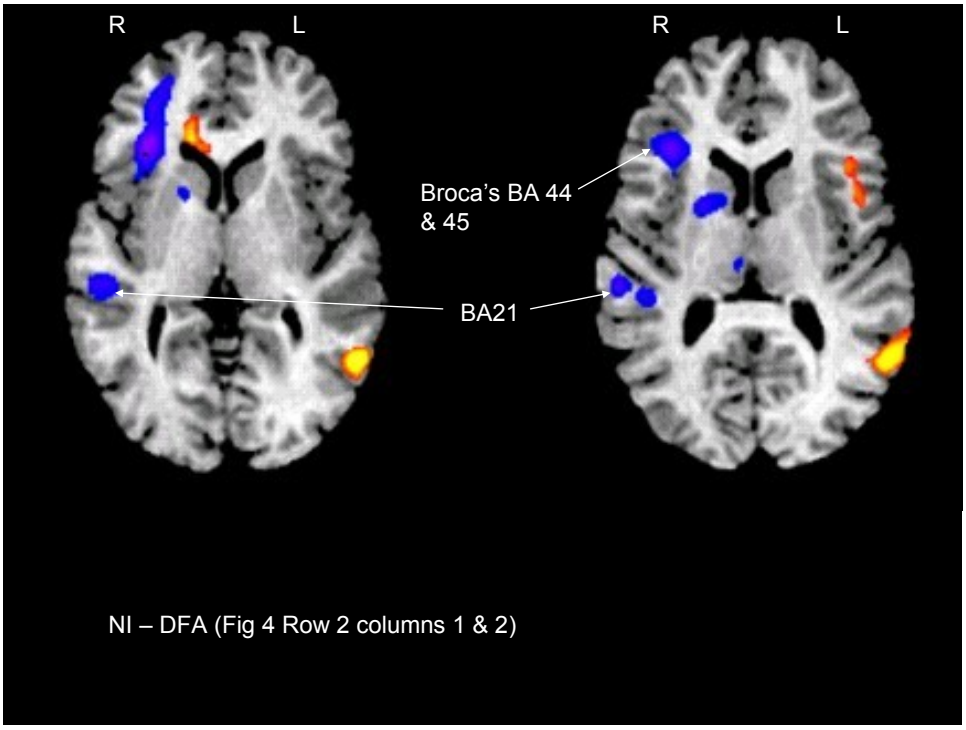

Figure 17. Location of significant differences in Regions of Interest. All regions identified in the figure have activation that is significantly higher for the DFA group than the NI group. (The image is an enlargement of the image presented in Figure 4, Row 2.

As can be seen in Figure 17 the DFA group exhibits higher activation in right hemisphere middle Temporal (functional BA 21) and Inferior Frontal (functional Broca's) regions. In addition, the left hemisphere differences identified in Figure 18 indicate higher activation in the occipital region (functional BA 19) by the DFA group and higher activation in by the NI group in parietal regions (functional BA 39).

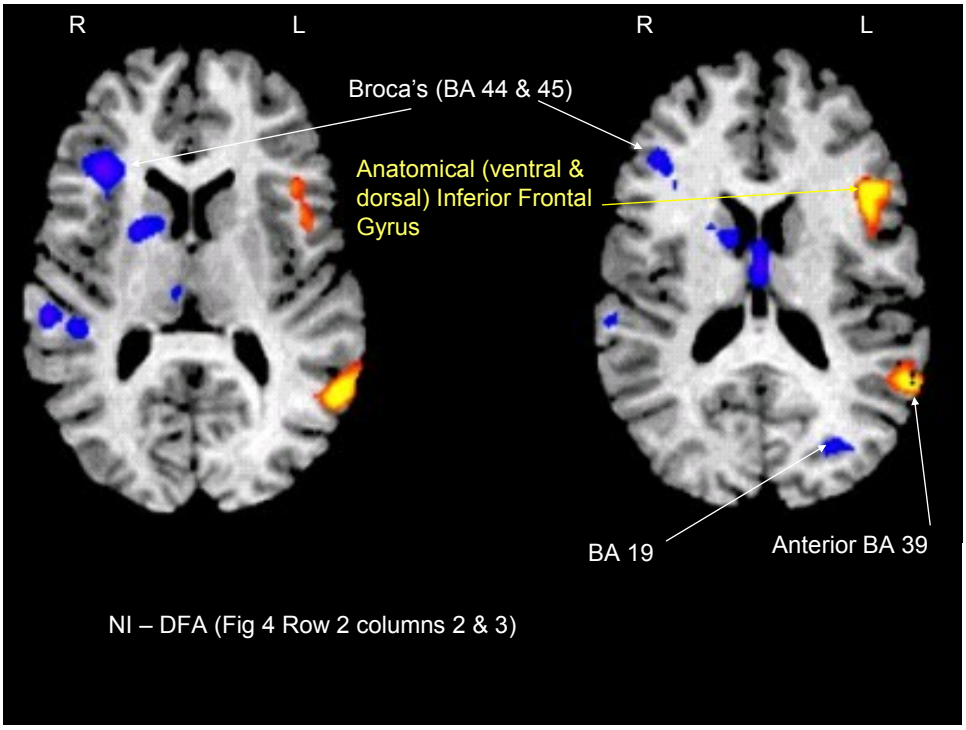

Figure 18. Location of significant differences in Regions of Interest. Regions in blue have activation that is significantly higher for the DFA group than the NI group. Regions in yellow-red have activation significantly higher for the NI group than the DFA group. (The image is an enlargement of the image presented in Figure 4, Row 2.)

Finally, The DFI and DFA groups exhibit differential activation in prefrontal cortex (functional BA10) shown in Figure 19. Activation by the DFA group is higher than that for the DFI group.

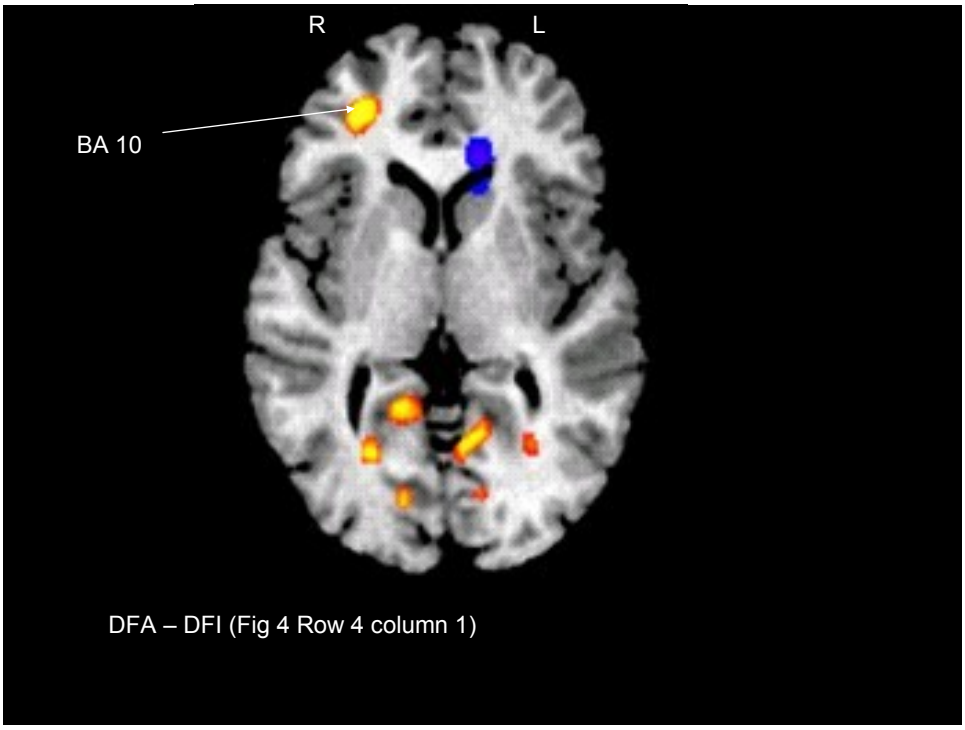

Figure 19. Location of significant difference in functional Brodmann Area 10. Activation is significantly higher for the DFA group than the DFI group. (The image is an enlargement of the image presented in Figure 4, Row 4.)

Discussion:

The results of the quantitative analyses of the functional and anatomical ROIs is generally consistent with previous findings from our research group. Specifically, greater activation in normal readers in anterior systems - left hemisphere inferior frontal regions (anatomical IFG) and posterior parietal regions (functional BA 39) combined with higher activations by DFA group in the other posterior system implicated in reading - the occipital region (functional BA 19) - demonstrating differential activation. (3,5,13,14) Of particular interest is the group of activations that distinguish the DFA group from the NI and DFI groups. Increased use of right hemisphere systems by the DFA group is

consistent with findings from readers who have compensated for phonological deficits in their early schooling. (13) Furthermore, increased activation of left hemisphere occipital systems by the DFA group further suggest a role for compensation made by those dysfluent readers with accurate decoding.

It should be noted that there is little consensus between the functional and anatomical ROIs that are in similar brain regions. Perhaps the strongest example of this lack of overlap is evident between the functionally defined Broca's region and the anatomically defined Inferior Frontal Region. Each approach yielded a separate significant finding (a right hemisphere difference for the functionally identified region and a left hemisphere difference for the anatomically derived region. Addressing this lack of consensus will be an important aspect of continuing research.

Conclusions:

The data from this study suggest that anatomically-based ROIs can be useful in identifying neural systems engaged by complex cognitive tasks. With continued improvement in imaging technology and analysis, taken together with better understanding of the neural systems engaged in both efficient and impaired reading, the precision and accuracy of both functionally- and anatomically-based localization of brain function will improve.

References

1. Shaywitz, S. (2003). Overcoming dyslexia: A new and complete science-based program for reading problems at any level. New York: Alfred A. Knopf.

2. Shaywitz, S., Mody, M., & Shaywitz, B. (2006). Neural mechanisms in dyslexia. Current Directions in Psychological Science, 15, 278-281.

3. Shaywitz, S, & Shaywitz, B. (2005). Dyslexia (specific reading disability). Biological Psychiatry, 57, 1301–1309.

4. Shaywitz, S. (1996). Dyslexia. Scientific American, 275, 98-104.

5. Shaywitz, B., Skudlarski, P., Holahan, J., et al. (2007). Age-related changes in reading systems of dyslexic children. Annals of Neurology, 61, 363-370.

6. Belliveau JW, Kennedy DN, McKinstry RC, Buchbinder BR, Weisskoff RM, Cohen MS, Vevea JM, Brady TJ, and Rosen BR (1991). "Functional mapping of the human visual cortex by magnetic resonance imaging". Science **254**: 716–719

7. Wiederholt, J. and B. Bryant (2002). Gray Oral Reading Tests 4th ed. Austin, TX, PRO-ED.

8. Torgesen, J.K., R.K. Wagner, and C.A. Rashotte, TOWRE: Test of Word Reading Efficiency. 1999, Austin: Pro-Ed.

9. Woodcock, R. W. and M. B. Johnson (1989). Woodcock-Johnson Psycho-Educational Battery--Revised (WJ-R). Allen, TX, Developmental Learning Materials.

10. The Psychological Corporation (1999): Wechsler Abbreviated Scale of Intelligence. San Antonio, TX: Harcourt Brace.

11. Nolf E, "XMedCon - An open-source medical image conversion toolkit"; European Journal of Nuclear Medicine; Vol. 30 (suppl. 2); 2003; pp S246; TP39

12. Duncan, J.S., Papademetris, X., et al Geometric Strategies for Neuroanatomic Analysis from MRI. NeuroImage 2004;23 Suppl 1:S34-45.

13. Shaywitz, B. A., Shaywitz, S. E., Pugh, K. R., Mencl, W. E., Fulbright, R. K., Skudlarski, P., et al. (2002). Disruption of posterior brain systems for reading in children with developmental dyslexia. *Biol Psychiatry, 52*(2), 101-110.

14. Shaywitz, S. E., Shaywitz, B. A., Fulbright, R. K., Skudlarski, P., Mencl, W. E., Constable, R. T., et al. (2003). Neural systems for compensation and persistence: young adult outcome of childhood reading disability. *Biol Psychiatry, 54*(1), 25-33.